Contents lists available at ScienceDirect

## Journal of Alloys and Compounds

journal homepage: www.elsevier.com/locate/jalcom



# Effect of time on the isothermal viscosity of metallic glass supercooled liquids



Akib Jabed, Chandra Sekhar Meduri, Golden Kumar\*

Department of Mechanical Engineering, The University of Texas at Dallas, Richardson, TX 75080, USA

#### ARTICLE INFO

Article history: Received 29 September 2020 Received in revised form 29 October 2020 Accepted 21 November 2020 Available online 25 November 2020

Keywords: Metallic glass Thermoplastic forming Supercooled liquid Crystallization

#### ABSTRACT

The viscosity of metallic glasses is considered to remain constant during thermoplastic forming operations. Here, we quantify the time dependent change in isothermal viscosity of Pt<sub>57.5</sub>Cu<sub>14.7</sub>Ni<sub>5.3</sub>P<sub>22.5</sub> and Zr<sub>35</sub>Ti<sub>30</sub>Cu<sub>8.25</sub>Be<sub>26.75</sub> glass formers in the supercooled liquid state. The samples were isothermally held prior to thermoplastic molding to probe the viscosity at different times. The viscosity values were extracted from the filling length of mold cavities. The viscosity increased with annealing time and the rate of increase was found to be largely independent of temperature and type of glass former. However, the viscosity increase was higher in the outer parts of samples which experienced higher shear rate during molding. Crystal nucleation and growth contributions are considered to explain the observed changes in effective viscosity of remaining amorphous phase. Our results suggest that thermoplastic forming is an effective tool in analyzing subtle changes in structure and viscosity of metallic glass supercooled liquids.

© 2020 Elsevier B.V. All rights reserved.

## 1. Introduction

The supercooled or undercooled liquid state of glass forming metallic alloys is of scientific and technological importance. Study of supercooled liquids has advanced our understanding of nucleation and growth of crystals in complex systems [1-7]. The glass forming ability (GFA) of an alloy is inherently related to the properties of its supercooled liquid state [8-10]. Higher viscosity of supercooled liquid improves GFA by decreasing the nucleation and growth rates [11–13]. The temperature range of supercooled liquid state has also been used to rationalize the GFA trends in metallic alloys [14].

In recent years, thermoplastic forming (TPF) has evolved as a precision manufacturing technique for metallic glass (MG) parts that are otherwise difficult to prepare by casting and machining [15–19]. Complex metallic microparts and surface patterns ranging from nanowires to hierarchical architectures can be fabricated by pressing the viscous MGs against templates [15-21]. Forming techniques other than embossing such as, powder consolidation [22], blow molding [23], rolling [24], and wire drawing [25,26] have also been demonstrated using the supercooled liquid state of MGs. TPF experiments with MGs are performed in the supercooled liquid state at a constant temperature where the crystallization time is several minutes [17,18]. The available processing time for TPF is determined

In this work, we investigate the effect of time on the viscosity and TPF of MG supercooled liquids at a constant temperature. Majority of the thermoplastic forming experiments with MGs are conducted in air, and therefore oxidation might also influence the effective viscosity of metallic liquids. To probe the effect of oxidation and crystallization on the isothermal viscosity of supercooled liquids, we

E-mail address: Golden.Kumar@UTDallas.edu (G. Kumar).

from the isothermal crystallization curves. Various models have been developed to describe the flow of MG supercooled liquids in TPF operations [27–31]. These models assume that the viscosity of MG supercooled liquid remains constant as a function of time and loading rate during TPF. However, it is well established that the metastable MG supercooled liquid continuously undergoes irreversible nucleation and growth even prior to detectable crystallization by calorimetric measurements [32–35]. It remains unclear if such early stages of crystallization affect the viscosity and TPF outcome of MGs. Understanding the time dependent viscous flow of MG is critical because the MGs are typically subjected to multiple sequential thermoplastic operations [21]. For example, the flat MG samples used as feedstock for thermoplastic imprinting are prepared by parallel plate thermoplastic pressing [18]. In addition to time, shear rate experienced by MG during TPF can also affect the viscosity. It has been shown that the shear rate can accelerate the crystallization of MG supercooled liquids [36]. Therefore, it is important to understand the combined effect of time and shear rate on the flow ability of MG supercooled liquids.

<sup>\*</sup> Corresponding author.

study Pt-based (inert) and Zr-based (prone to oxidation) MG formers.

## 2. Material and methods

Pt<sub>57.5</sub>Cu<sub>14.7</sub>Ni<sub>5.3</sub>P<sub>22.5</sub> (Pt-based) ingot was prepared by melting 99.9% pure elements in a vacuum-sealed quartz tube. The ingot was fluxed with B<sub>2</sub>O<sub>3</sub> to remove the oxide impurities. A MG rod with a diameter of about 2 mm was produced by water quenching. The quenched sample was characterized using TA Instruments 25P differential scanning calorimeter (DSC) to verify the glassy state. The constant heating rate DSC curves for Pt-based and Zr-based MGs are included in the Supplementary Information (Fig. S1). The glass transition temperature ( $T_g$ ) and the onset temperature of crystallization ( $T_x$ ) for Pt-based MG were 230 °C and 305 °C, respectively. Zr<sub>35</sub>Ti<sub>30</sub>Cu<sub>8.25</sub>Be<sub>26.75</sub> (Zr-based) MG rod of 10 mm diameter was purchased from the Liquidmetal Technologies. The  $T_g$  and  $T_x$  of Zr-based MG were measured to be 320 °C and 465 °C, respectively.

To probe the viscosity at different times, the MGs were isothermally annealed for varying times followed by thermoplastic embossing at the same temperature. The temperatures for isothermal experiments were selected such that the time for onset of crystallization was several minutes to replicate the conditions used in TPF. To ensure reproducibility in embossing results, the as-cast MG samples were thermoplastially pre-pressed in the form of discs of 3 mm diameter and 0.5 mm thickness. The discs were annealed in DSC to minimize the temperature fluctuation. The embossing experiments were performed against silicon molds containing cylindrical cavities. The cavities of 20 µm diameter with center-to-center spacing of 100 µm and 25 µm diameter with center-to-center spacing of 50 µm were prepared by photolithography and deep-reactive-ion-etching. Custom-made heating plates were installed on Instron mechanical testing machine to conduct the controlled embossing experiments. After placing the MG disc on silicon template, the load was increased to 250 N at a rate of 500 N/min followed by immediate unloading. The entire thermoplastic embossing step lasted about 1 min for each sample. The silicon was etched away in KOH and the MG samples were characterized by Zeiss Supra 40 scanning electron microscope (SEM). The length of MG micropillars was measured at different distances from the center of the sample because the pressure and shear rate vary with location in parallel plate embossing. The viscosity of MG supercooled liquid was extracted from the length of micropillars using the lubrication model for thermoplastic embossing [27].

#### 3. Results and discussion

Fig. 1 shows isothermal DSC curves of Pt-based MG at 260 °C and 270 °C and Zr-based MG at 410 °C. The onset time for crystallization  $(t_x)$  determined by intersection of tangents for Pt-based MG is 45 min at 260 °C, 20 min at 270 °C, and for Zr-based MG the  $t_x$  is 14 min at 410 °C. The crystal fraction at  $t_x$  is proposed to reach about 1% in previous isothermal studies on MGs. Therefore, the viscosity of MG supercooled liquids is generally assumed to remain unchanged until  $t_x$ . To test this hypothesis, the Pt-based and Zr-based MGs were isothermally annealed and embossed at three temperatures shown in Fig. 1. The arrows indicate the annealing times before thermoplastic embossing at respective temperatures.

Fig. 2 shows the SEM images of Pt-based and Zr-based MGs thermoplastically embossed after annealing for different times. The SEM images are taken from the center of the samples to allow a direct comparison between the micropillar lengths. It is evident that the micropillar length decreases with increasing annealing time for both MGs. The change in length is more noticeable when the annealing time approaches  $t_x$ . Similar trend in micropillar length is observed for two different annealing temperatures for the Pt-based

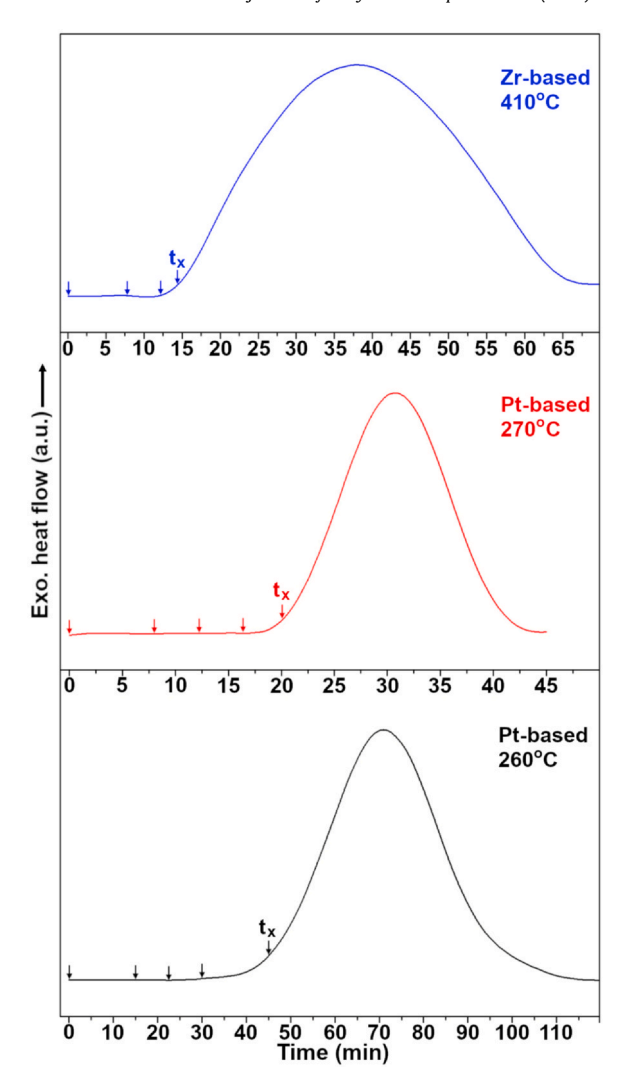


**Fig. 1.** Isothermal DSC curves of Zr-based and Pt-based MGs. The arrows mark the annealing times used prior to thermoplastic forming. The  $t_x$  is the time for onset of isothermal crystallization.

MG. The filling of microscale cavities with MG supercooled liquid depends on the pressure, the cavity size, and the viscosity of liquid. The observed change in length of micropillars indicates change in viscosity during isothermal annealing because the other parameters were kept constant.

The lengths of micropillars were measured from the SEM images to quantify the flow ability of supercooled liquid as a function of isothermal annealing time. Three different locations in each sample were analyzed because the pressure and the shear rate are not uniform in the disc during parallel plate squeezing [27,36]. To decouple the pressure effect, the filling length was considered 100% for an unannealed sample at every location. The normalized filling length for Pt-based MG at 260 °C and 270 °C is plotted in Fig. 3. The length gradually decreases with annealing time and reaches 50% in the center of the samples (r = 0 mm, where r is the distance from the center) at the onset time of crystallization. The decreasing filling length is an indicator of increase in viscosity during isothermal annealing. Therefore, the flow ability of MG supercooled liquids is sensitive to the thermal history. The outer parts are affected more than the center of the samples by isothermal annealing (Fig. 3). The filling length reduces to about 30% at the periphery of the samples (r=2 mm). The difference in filling length at the center and the periphery grows with increasing annealing time. Similar trend in

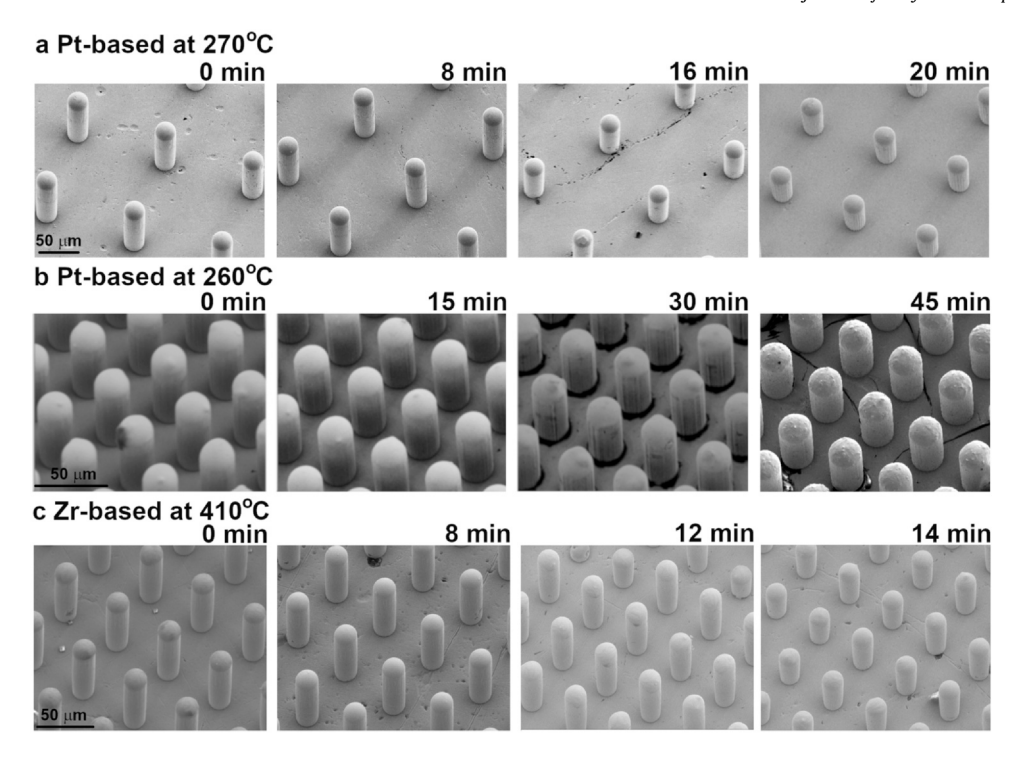
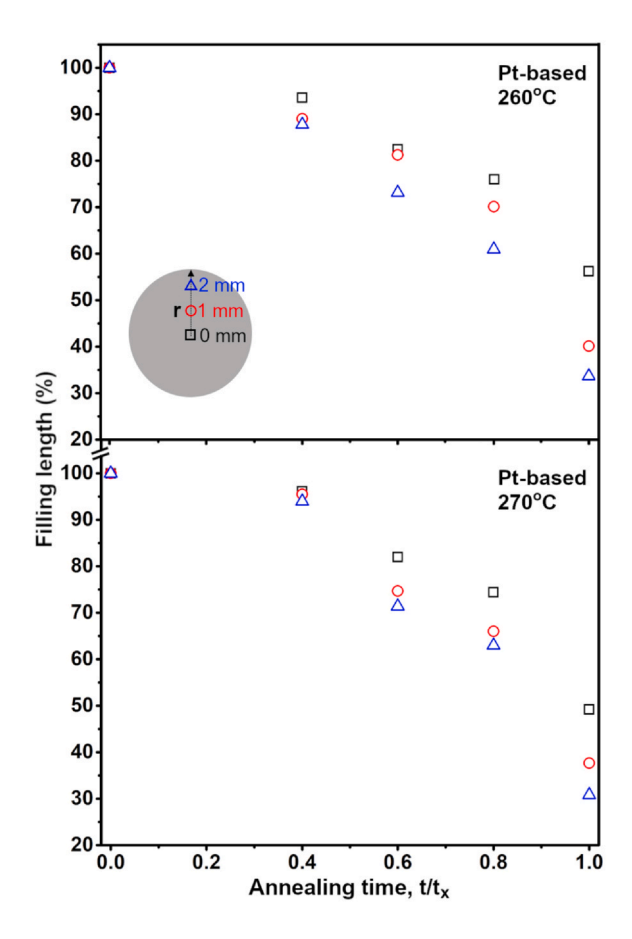


Fig. 2. The SEM images of MG micropillars prepared by thermoplastic embossing after isothermal annealing for different times. All images are taken from the center of the samples. The pillar length decreases with annealing time in all cases.



**Fig. 3.** The filling length for Pt-based MG as a function of annealing time at two different temperatures. The filling length at three locations in the circular samples are plotted. The values are normalized with respect to the filling length for unannealed samples.

filling length was observed for the Zr-based MG after isothermal annealing at 410 °C (Supplementary Information Fig. S3). It has been shown that the shear rate can accelerate crystallization in MG supercooled liquids [36]. The shear rate ( $\dot{\gamma}$ ) in parallel plate embossing of disc increases with r as:

$$\dot{\gamma} = \frac{3\dot{h}}{\sqrt{2}h} \left[ \left( \frac{rz}{h^2} \right)^2 + 3\left( 1 - \left( \frac{z}{h} \right)^2 \right) \right]^{\frac{1}{2}} \tag{1}$$

Where h is the half thickness of disc and z coordinate is measured from the center of the mid plane. The previous study showed that the outer parts of thermoplastically embossed MG discs exhibit shorter isothermal crystallization time [36]. Thus, the lower filling observed at the periphery of samples in our experiments is a combined effect of annealing time and higher shear rate on the viscosity.

Lubrication model was used to extract the viscosity values from the filling length of MG samples [27]. The procedure is briefly described in Supplementary Information. The value of viscosity for unannealed Ptbased MG at 270 °C was estimated to be  $7 \times 10^6$  Pas which is close to 1.4 × 10<sup>7</sup> Pa's calculated using the VFT (Vogel-Fulcher-Tammann) parameters reported in literature [37]. Therefore, the lubrication approach works reasonably well for measuring the relative change in viscosity of MG supercooled liquids as a function of annealing time. Fig. 4 shows the normalized viscosity values for Pt-based (at 260 °C and 270 °C) and Zrbased (at 410 °C) MGs as a function of annealing time. The viscosity increases with annealing time in all three cases. The viscosity at the outer parts is consistently higher than at the center of the samples due to shear-induced crystallization. The viscosity difference is higher in Zrbased MG indicating its higher sensitivity to shear rate. The initial increase in viscosity in all three cases is less than a factor of two for annealing up to about  $0.4t_x$ . At longer annealing times, the rate of change in viscosity is higher and the overall increase is five to six times in the entire supercooled range. The viscosity increase in Pt-based MG is lower at 260 °C compared to at 270 °C. There is no noticeable effect of oxidation as the increase in viscosity of Zr-based MG is comparable to the

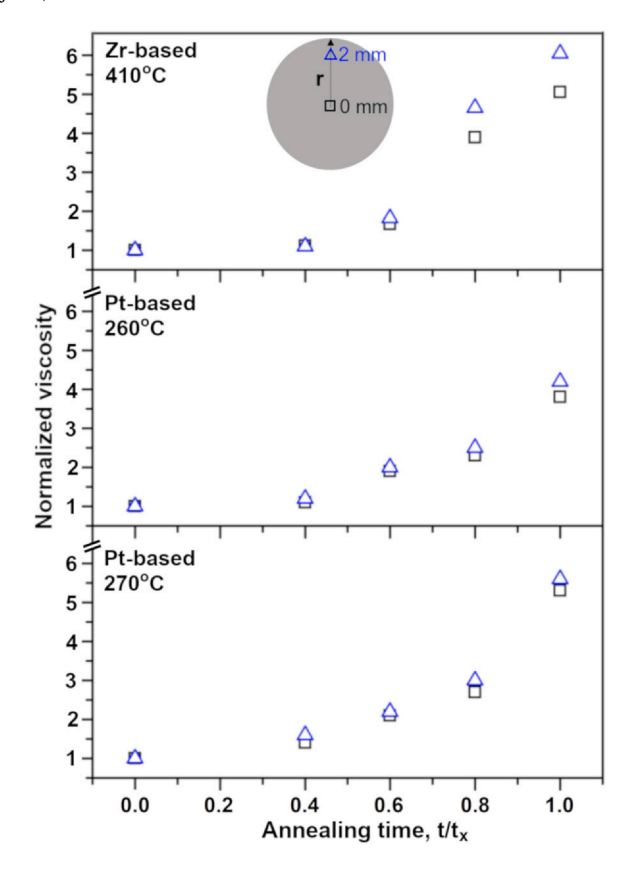


**Fig. 4.** The time dependent change in normalized viscosity of MG supercooled liquids calculated from the filling length of annealed MGs. The values at the center and the periphery of samples are shown.

Pt-based MG. The time dependence of viscosity follows the kinetics of phase transformation controlled by nucleation and growth. In the following section, we analyze the fraction of crystallization during annealing and its effect on the effective viscosity.

The MG samples after isothermal annealing were characterized by constant heating rate DSC. The DSC curves of Pt-based MG after isothermal annealing for varying times at 270 °C are shown in Fig. 5. The DSC of unannealed sample is also shown for comparison. The  $T_{\sigma}$ 

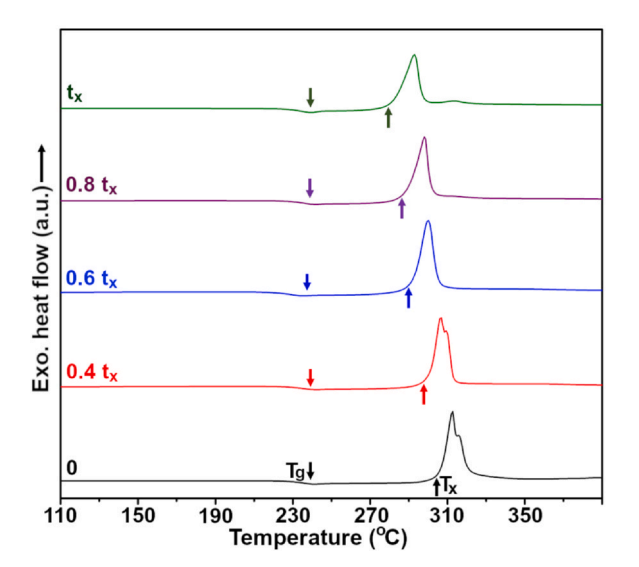


**Fig. 5.** The constant heating rate DSC curves of Pt-based MG samples annealed and embossed at 270 °C. The onset temperature of crystallization  $(T_x)$  decreases with annealing.

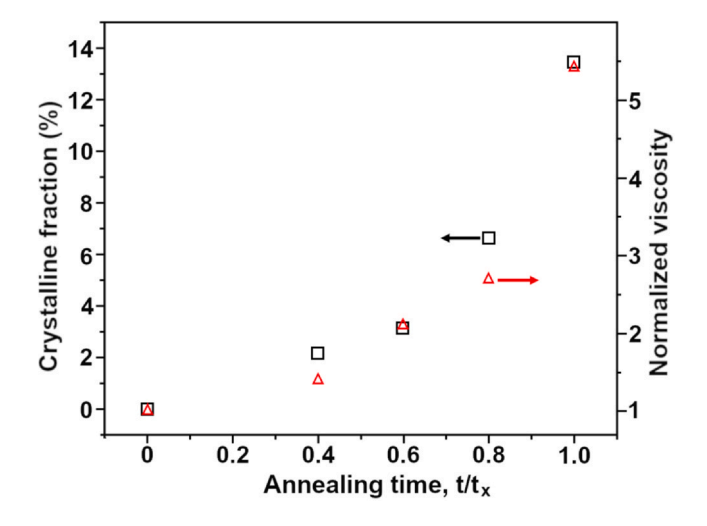


**Fig. 6.** Comparison of crystalline fraction and viscosity of Pt-based MG as function of annealing time at 270 °C. The crystal fraction was calculated from the DSC curves (Fig. 5) and viscosity values are taken from Fig. 4.

remains unaffected by annealing but the onset of crystallization shifts to lower temperature with increasing annealing time. The decrease in crystallization temperature is an indicator of decreased thermal stability of the supercooled liquid state. This is typically observed when the MG is partially crystalline [38]. The area of crystallization peak decreases with annealing time, which also suggests the change in fraction of amorphous and crystalline phases during annealing.

The amount of crystalline phase can be calculated from the enthalpy of crystallization by considering the unannealed sample to be 100% amorphous. The crystalline fraction and viscosity values for Ptbased MG are plotted together as a function of annealing time at 270 °C (Fig. 6). The fraction of crystalline phase increases with annealing time and reaches about 13% at the onset of crystallization. The XRD patterns shown in Supplementary Information (Fig. S2) confirm the formation of crystalline phase after annealing for 20 min at 270 °C. The viscosity and the crystal fraction show similar annealing time dependence indicating a direct correlation. Typically, the crystal fraction is assumed to be about 1% at the onset of isothermal crystallization in MGs [39]. However, our experimental results suggest significantly higher fraction of crystalline phase in isothermally annealed and embossed samples. It is unlikely for the viscosity to increase by five to six times due to 1% crystalline phase. It is important to note that Einstein's model [40] for viscosity of mixtures predicts less than 20% increase in effective viscosity of a liquid that contains 13% solid particles. Therefore, the increase in viscosity of 5-6 times during isothermal annealing of MGs cannot be attributed only to the presence of 10–15% crystalline phase. Previous studies have reported substantial increase in isothermal viscosity of Zr-based MGs which relax, and phase separate in the supercooled liquid state [41-43]. Although, no phase separation has been reported in the MG formers considered in present work but change in composition is expected during non-polymorphic crystallization. Therefore, the increase in viscosity during isothermal annealing observed in present work is a combined effect of crystalline phase and change in fluidity of the remaining amorphous matrix.

Isothermal crystallization of MGs occurs by nucleation and growth processes and can be modeled using Johnson-Mehl-Avarami-Kolmogorov theory [39]. The fraction of crystalline phase increases slowly in the nucleation stage followed by rapid increase in the growth stage. Similar time dependence of crystal fraction and viscosity (Fig. 6) suggests that the nucleation has lesser effect on the viscosity of MG than the growth. This can explain why the MG in its as-prepared state exhibits reproducible flow characteristics despite

containing different distribution of nuclei. The growth of crystals with significantly different composition from the amorphous matrix requires redistribution of elements. Therefore, increase in isothermal viscosity of MG supercooled liquids is predominantly due to change in composition of remaining amorphous phase caused by the growth of chemically distinct crystalline phases.

#### 4. Conclusions

We investigated the time dependence of isothermal viscosity of Pt-based and Zr-based metallic glasses in the supercooled liquid state using thermoplastic forming. The results show that the isothermal viscosity of MG supercooled liquids does not remain constant. The variation of viscosity follows the kinetics of a typical phase transformation controlled by nucleation and growth. The viscosity increases slowly in the nucleation stage followed by rapid increase due to growth. The increase in viscosity is attributed to the combined effect of compositional redistribution in the amorphous phase and the presence of crystalline phase. The overall increase in viscosity of MG is about six times in the supercooled liquid range. The higher shear rate at the periphery of samples results in additional increase in viscosity due to shear induced structural changes. The effect of oxidation on viscosity of MG supercooled liquid is less significant and can be ignored for microscale embossing. Thermoplastic processing time for metallic glasses should be less than 40% of the crystallization time to produce predominantly amorphous structures.

#### **CRediT authorship contribution statement**

**Akib Jabed**: Experimentation, Data Analysis, Draft Preparation. **Chandra Sekhar Meduri**: Data Analysis, Editing. **Golden Kumar**: Project Supervision, Final Writing and Revision of Manuscript.

## **Declaration of Competing Interest**

The authors declare that they have no known competing financial interests or personal relationships that could have appeared to influence the work reported in this paper.

## Acknowledgements

The work was supported by the US National Science Foundation (NSF) through Award #1919445 and NSF-CAREER Award #1921435.

## Appendix A. Supporting information

Supplementary data associated with this article can be found in the online version at doi:10.1016/j.jallcom.2020.158067.

## References

- [1] J.C. Fisher, J.H. Hollomon, D. Turnbull, Rate of nucleation of solid particles in a subcooled liquid, Science 109 (1949) 168–169.
- [2] D. Turnbull, J.C. Fisher, Rate of nucleation in condensed systems, J Chem. Phys. 17 (1949) 71–73.
- [3] H.S. Chen, D. Turnbull, Atmospheric corrosion of splat cooled aluminum alloy foils, JOM 20 (1968) 10–11.
- [4] H. Fecht, W.L. Johnson, Thermodynamic properties and metastability of bulk metallic glasses, Mater. Sci. Eng. A 375 (2004) 2–8.
- [5] J.Z. Jiang, C.H. Jensen, A.R. Rasmussen, Time-dependent nucleation in undercooled Pd43Cu27Ni10P20, Metastable, Mech. Alloy. Nanocryst. Mater. (2003) 91, 96.
- [6] H. Assadi, J. Schroers, Crystal nucleation in deeply undercooled melts of bulk metallic glass forming systems, Acta. Mater. 50 (2002) 89–100.
- [7] K.F. Kelton, Nucleation in silicate and metallic glasses, Int. J. Non-Equilib. Process. 11 (1998) 141–168.
- [8] M. Marcus, D. Turnbull, Correlation between glass-forming tendency and liquidus temperature in metallic alloys, Mater. Sci. Eng. 23 (1976) 211–214.

- [9] H.W. Kui, A.L. Greer, D. Turnbull, Formation of bulk metallic-glass by fluxing, Appl. Phys. Lett. 45 (1984) 615–616.
- [10] R. Busch, A. Masuhr, E. Bakke, W.L. Johnson, Strong liquid behavior of Zr-Ti-Cu-Ni-Be bulk metallic glass forming alloys, Mater. Res. Soc. Sym. Proc. 455 (1997) 369–374.
- [11] S. Mukherjee, J. Schroers, Z. Zhou, W.L. Johnson, W.K. Rhim, Viscosity and specific volume of bulk metallic glass-forming alloys and their correlation with glass forming ability, Acta. Mater. 52 (2004) 3689–3695.
- [12] K.F. Kelton, Influence of microalloying on glass formation and crystallization, J. Alloy. Compd. 434 (2007) 115–118.
- [13] W.L. Johnson, Bulk glass-forming metallic alloys: science and technology, MRS Bull. 24 (1999) 42–56.
- [14] A. Inoue, Stabilization of metallic supercooled liquid and bulk amorphous alloys, Acta. Mater. 48 (2000) 279–306.
- [15] Y. Saotome, Y. Fukuda, I. Yamaguchi, A. Inoue, Superplastic nanoforming of optical components of Pt-based metallic glass, J. Alloy. Compd. 434 (2007) 97–101.
- [16] J. Schroers, Q. Pham, A. Desai, Thermoplastic forming of bulk metallic glass a technology for MEMS and microstructure fabrication, J. Microelectromech. Syst. 16 (2007) 240–247.
- [17] J. Schroers, Processing of bulk metallic glass, Adv. Mater. 22 (2010) 1566–1597.
- [18] G. Kumar, A. Desai, J. Schroers, Bulk metallic glass: the smaller the better, Adv. Mater. 23 (2011) 461–476.
- [19] L. Liu, M. Hasan, G. Kumar, Metallic glass nanostructures: fabrication, properties, and applications, Nanoscale 6 (2014) 2027–2036.
- [20] G. Kumar, H. Tang, J. Schroers, Nanomoulding with amorphous metals, Nature 457 (2009) 868–872.
- [21] M. Hasan, J. Schroers, G. Kumar, Functionalization of metallic glasses through hierarchical patterning, Nano Lett. 15 (2015) 963–968.
- [22] B. Bochtler, M. Stople, B. Reiplinger, R. Busch, Consolidation of amorphous powder by thermoplastic forming and subsequent mechanical testing, Mater. Des. 140 (2018) 188–195.
- [23] J. Schroers, T.M. Hodges, G. Kumar, H. Raman, A.J. Barnes, Q. Pham, T.A. Waniuk, Thermoplastic blow molding of metals, Mater. Today 14 (2011) 14–19.
- [24] R. Martinez, G. Kumar, J. Schroers, Hot rolling of bulk metallic glass in its supercooled liquid region, Scr. Mater. 59 (2008) 187–190.
- [25] M. Hasan, G. Kumar, High-throughput drawing and testig of metallic glass nanostructures, Nanoscale 9 (2017) 3261–3568.
- [26] Z. Hu, C.S. Meduri, J. Blawzdziewicz, G. Kumar, Nanoshaping of glass forming metallic liquids by stretching: evading lithography, Nanotechnology 30 (2018) 075302.
- [27] G. Kumar, J. Schroers, J. Blawzdziewicz, Controllable nanoimprinting of metallic glasses: effect of pressure and interfacial properties, Nanotechnology 24 (2013) 105301.
- [28] Z. Li, Z. Huang, F. Sun, X. Li, J. Ma, Forming of metallic glasses: mechanisms and processes. Mater. Today Adv. 7 (2020) 100077.
- [29] B. Bochtler, O. Kruse, R. Busch, Thermoplastic forming of amorphous metals, J. Phys.: Condens. Matter 32 (2020) 244002.
- [30] N. Zhang, J.S. Chu, C.J. Byrne, D.J. Browne, M.D. Gilchrist, Replication of micro/nano-scale features by micro injection molding with a bulk metallic glass mold insert, J. Micromech. Microeng. 22 (2012) 065019.
- [31] N. Li, W. Chen, L. Liu, Thermoplastic micro-forming of bulk metallic glasses: a review, JOM 68 (2016) 1246–1261.
- [32] J. Schroers, R. Busch, S. Bossuyt, W.L. Johnson, Crystallization behavior of the bulk metallic glass forming Zr41Ti14Cu12Ni10Be23 liquid, Mater. Sci. Eng. A 304 (2001) 287–291.
- [33] J.H. Perepezko, Nucleation-controlled reactions and metastable structures, Prog. Mater. Sci. 49 (2004) 263–284.
- [34] Q.S. Zhang, Y.F. Deng, L.L. He, H.F. Zhang, B.Z. Ding, Z.Q. Hu, Isothermal nanocrystallization of Zr55Al10Ni5-Cu-30 bulk amorphous alloy near the glass transition temperature, Acta. Metall. Sin. 39 (2003) 301–304.
- [35] T. Waniuk, J. Schroers, W.L. Johnson, Timescales of crystallization and viscous flow of the bulk glass-forming Zr-Ti-Ni-Cu-Be alloys, Phys. Rev. B 67 (2003) 184203.
- [36] Z. Shao, J.P. Singer, Y.H. Liu, Z. Liu, H.P. Li, M. Gopinadhan, C.S. O'Hern, J. Schroers, C.O. Osuji, Shear-accelerated crystallization in a supercooled atomic liquid, Phys. Rev. E 91 (2015) 020301.
- [37] B.A. Legg, J. Schroers, R. Busch, Thermodynamics, kinetics, and crystallization of Pt57.3Cu14.6Ni5.3P22.8 bulk metallic glass, Acta Mater. 55 (2007) 1109–1116.
- [38] G. Kumar, T. Ohkubo, K. Hono, Effect of melt temperature on the mechanical properties of bulk metallic glasses, J. Mater. Res. 24 (2009) 2353–2360.
- [39] O. Gross, S.S. Riegler, M. Stolpe, B. Bochtler, A. Kuball, S. Hechler, R. Busch, I. Gallino, On the high glass-forming ability of Pt-Cu-Ni/Co-P-based liquids, Acta. Mater. 141 (2017) 109–119.
- [40] A. Eeinstein, Berichtigung zu meiner Arbeit: Eine neue Bestimmung der Moleküldimensionen, Ann. Phys. 339 (1911) 591–592.
- [41] E. Bakke, R. Busch, W.L. Johnson, The viscosity of the Zr46.75Ti8.25Cu7.5Ni10B e27.5bulk metallic glass forming alloy in the supercooled liquid, Appl. Phys. Lett. 67 (1995) 3260–3262.
- [42] T.A. Waniuk, R. Busch, A. Masuhr, W.L. Johnson, Equilibrium viscosity of the Zr41.2Ti13.8Cu12.5Ni10Be22.5 bulk metallic glass-forming liquid and viscous flow during relaxation, phase separation, and primary crystallization, Acta Mater. 46 (1998) 5229–5236.
- [43] R. Busch, E. Bakke, W.L. Johnson, Viscosity of the supercooled liquid amd relaxation at the glass transition of the Zr46.75Ti8.25Cu7.5Ni10Be27.5 bulk metallic glass forming aloy, Acta Mater. 46 (1998) 4725–4732.